Crystal Structure, NQR and DSC Studies of Tetrabromocadmates(II): $[4\text{-}H_2NC_5H_4NH]_2CdBr_4 \cdot H_2O$ and $[2,3,5,6\text{-}(CH_3)_4C_4N_2H_2]CdBr_4$

Naoko Hatano[a], Michio Nakashima[a], Keizo Horiuchi[b], Hiromitsu Terao[c],
and Hideta Ishihara[a]

[a] Faculty of Culture and Education, Saga University, Saga 840-8502, Japan
[b] Faculty of Science, University of the Ryukyus, 1 Senbaru, Okinawa 903-0213, Japan
[c] Faculty of Integrated Arts and Sciences, Tokushima University, Tokushima 770-8502, Japan

Reprint requests to Prof. H. Ishihara. E-mail: isiharah@cc.saga-u.ac.jp

Z. Naturforsch. **2008**, *63b,* 1181 – 1186; received May 26, 2008

4-Aminopyridinium tetrabromocadmate(II) monohydrate (**1**) crystallizes in the orthorhombic space group *Pbcm* with a = 6.876(2), b = 14.089(2), and c = 18.845(2) Å, Z = 4, T = 296 K. In the crystal structure, a $[CdBr_4]^{2-}$ anion, a 4-aminopyridinium cation, and a water molecule are alternately connected into chains by hydrogen bonds N–H···Br and O–H···Br. 2,3,5,6-Tetramethylpyrazinium tetrabromocadmate(II) (**2**) crystallizes in the orthorhombic space group $P2_12_12_1$ with a = 14.640(12), b = 15.615(7), c = 6.686(5) Å, Z = 4, T = 296 K. In the crystal structure, a $[CdBr_4]^{2-}$ anion and a 2,3,5,6-tetramethylpyrazinium cation are interconnected by bifurcated hydrogen bonds N–H···2Br and form infinite chains. ^{81}Br NQR spectra with three lines with an intensity ratio of 1 : 1 : 2 (77 K $\leq T \leq$ *ca.* 325 K) and four lines with an intensity ratio of 1 : 1 : 1 : 1 (77 K $\leq T \leq$ *ca.* 330 K) were observed for crystalline **1** and **2**, respectively, which are consistent with the crystal structure data. DSC measurements showed the existence of thermal anomalies at high temperatures in both **1** and **2**.

Key words: Crystal Structure, Tetrabromocadmate(II), DSC, NQR

Introduction

The formation of halogenocadmates(II) with a variety of cations is well known, and we found the crystal structures of their salts with simple ammonium ions to be quite diverse depending on the cations [1 – 8]. These structures can be divided coarsely into two groups: discrete anions and infinitely polymerized ones. Distorted tetrahedral CdX_4^{2-} ions [1, 2] are found in the structures of R_2CdX_4 (R = univalent cation, X = halogen). Infinitely polymerized anions, which are one-dimensional chains or two-dimensional sheets, are formed through secondary Cd···X bonds. One-dimensional chains [3 – 5] are found in the structures of complexes of RCdX$_3$, R_3CdX$_5$, RCd$_2$X$_5$, and R_4Cd$_3$X$_{10}$. The chains of $[CdX_3^{-}]_\infty$ are formed among CdX$_5$ trigonal bipyramids sharing two edges, and those of $[CdX_5^{3-}]_\infty$ from CdX$_6$ octahedra sharing two corners. The more complex chains of $[Cd_2X_5^{-}]_\infty$ and $[Cd_3X_{10}^{4-}]_\infty$ consist of CdX$_6$ octahedra sharing four edges and face-connected CdX$_6$ octahedra, respectively. Two-dimensional sheets [6] found for the R_2CdX$_4$ complexes are formed through CdX$_6$ octahedra sharing four corners.

The architectures and the stability of the crystals seem to be delicately dependent on the cation shapes and their formation of hydrogen bonds N–H···X. The members of the isomorphic series $[N(CH_3)_4]_2[MX_4]$ (M = Zn, Cd, Hg; X = Cl, Br, I) crystallize with discrete MX_4^{2-} anions. All these crystals undergo characteristic phase transitions related to the cation reorientation, and the transition temperatures are inversely proportional to the unit cell volumes [7]. Another isomorphic series of compounds, $[C_4H_{12}N_2][MX_4]$ (M = Zn, Cd, Hg; X = Br, I) also crystallizes with MX_4^{2-} anions, but the crystals have remarkable stability without exhibiting any phase transitions up to around 550 K, which was explained by well developed N–H···X hydrogen bond networks in the crystalline state [8]. On the other hand, $[H_3N(CH_2)_3NH_3][CdBr_4]$ and $[n\text{-}CH_3\text{-}CH_2CH_2NH_3]_2[CdBr_4]$ crystallize in two-dimensional perovskite-type layer structures based on CdBr$_6$ octahedra [6]. The cations are fitted into the rectangular cavities of the layers. A similar structure has also been seen in $[H_3NC_6H_4NO_2]_2[CdCl_4]$ [12] which is an ag-

0932–0776 / 08 / 1000–1181 $ 06.00

Table 1. Crystal structure data for **1** and **2**.

	1	**2**
Formula	$C_{10}H_{16}CdBr_4ON_4$	$C_8H_{14}CdBr_4N_2$
M_r	640.29	570.25
Cryst. size, mm^3	$0.37 \times 0.37 \times 0.22$	$0.30 \times 0.30 \times 0.80$
Crystal system	orthorhombic	orthorhombic
Space group	*Pbcm*	$P2_12_12_1$
a, Å	6.876(2)	14.640(12)
b, Å	14.089(2)	15.615(7)
c, Å	18.845(2)	6.686(5)
V, Å^3	1825.7(5)	1528.4(18)
Z	4	4
$D_{\text{calcd.}}$, g cm^{-3}	2.329	2.478
Temperature, K	296(1)	296(2)
$\mu(\text{Mo}K_\alpha)$, cm^{-1}	99.79	118.95
$F(000)$, e	1200	1056
hkl range	+8, +18, +24	+19, −20, +8
$((\sin\theta)/\lambda)_{\max}$, Å^{-1}	0.6497	0.6497
Refl. measured	2160	2026
Refl. unique $[I \geq 3\sigma(I)]$	991	1001
Param. refined	104	146
$R(F)/wR(F^2)$[a] $[I \geq 3\sigma(I)]$	0.049/0.062	0.099/0.115
x(Flack)	–	−0.00(14)
GoF (F)	2.07	5.15
$\Delta\rho_{\text{fin}}$(max/min), e Å^{-3}	0.82/−1.37	3.16/−2.84

[a] $R = \|F_o| - |F_c\|/|F_o|$, $wR = [\Sigma w(|F_o| - |F_c|)^2/\Sigma w F_o{}^2]^{1/2}$.

gregate with a cyclic molecular cation. As an extension of our former work we now employed 4-aminopyridinium and tetramethylpyrazinium ions for which some specific N–H···X hydrogen bonds may be expected in the crystalline state. The preparation, crystal structures, and the results of NQR and DSC measurements for $[4\text{-}H_2NC_5H_4NH]_2CdBr_4 \cdot H_2O$ and $[2,3,5,6\text{-}(CH_3)_4C_4N_2H_2][CdBr_4]$ are reported in this paper.

Results and Discussion

4-Aminopyridinium tetrabromocadmate(II) monohydrate $[4\text{-}H_2NC_5H_4NH]_2[CdBr_4] \cdot H_2O$ (1)

The crystal structure data of **1** are given in Table 1 [9]. The bond lengths, angles and short contacts are listed in Table 2. Fig. 1 shows a projection of the unit cell along [100] onto the *bc* plane, in which the asymmetric unit includes a 4-aminopyridinium cation, one half of a $CdBr_4{}^{2-}$ anion, and one half of a water molecule. The crystal structure consists of inorganic and organic columns stacked parallel to the *b* axis. In the former columns, $CdBr_4{}^{2-}$ tetrahedra and water molecules alternate. In the latter ones, 4-aminopyridinium cations are piled up by having their ring planes parallel but with alternating orientation. The $CdBr_4{}^{2-}$ anion is slightly distorted with bond lengths and angles as listed in Table 2.

Table 2. Selected bond lengths (Å), bond angles (deg), and short interatomic contacts (Å) in **1** and **2**.

$[4\text{-}H_2NC_5H_4NH]_2CdBr_4 \cdot H_2O$ (**1**)			
Cd–Br(1)	2.564(5)	Br(1)–Cd–Br(2)	106.5(1)
Cd–Br(2)	2.578(6)	Br(1)–Cd–Br(3)	109.7(1)
Cd–Br(3)	2.587(3)	Br(2)–Cd–Br(3)	109.8(1)
N(1)–C(1)	1.35(3)	N(1)–C(1)–C(2)	122(2)
N(1)–C(5)	1.33(3)	N(1)–C(5)–C(4)	125(2)
N(2)–C(3)	1.28(2)	C(1)–C(2)–C(3)	122(2)
C(1)–C(2)	1.29(3)	C(5)–C(4)–C(3)	118(2)
C(2)–C(3)	1.42(2)	N(2)–C(3)–C(2)	121(2)
C(3)–C(4)	1.42(2)	N(2)–C(3)–C(4)	124(2)
C(4)–C(5)	1.33(2)	C(2)–C(3)–C(4)	115(2)

Short contacts in **1**[a]

Connection	d(N···O/Br)	d(H···O/Br)	∠(N–H···O/Br)
N(1)–H(5)···O(1)[#1]	2.84(2)	1.92	163
N(2)–H(7)···Br(2)	3.60(2)	2.69	159
N(2)[#2]–H(6)[#2]···Br(2)	3.65(2)	2.76	158
N(2)[#3]–H(6)[#3]···Br(1)	3.47(2)	3.05	109
Br(1)···O(1)	3.47		
Br(2)···O(1)	3.66		
Br(3)···O(1)	3.49, 3.77		

[a] #1: $1-x$, $-y$, $1/2+z$; #2: x, $1/2-y$, $-1/2+z$; #3: $x-1$, y, z.

$[(CH_3)_4C_4N_2H_2]CdBr_4$ (**2**)			
Cd–Br(1)	2.564(5)	Br(1)–Cd–Br(2)	113.5(2)
Cd–Br(2)	2.577(6)	Br(1)–Cd–Br(3)	108.0(3)
Cd–Br(3)	2.587(7)	Br(1)–Cd–Br(4)	107.3(3)
Cd–Br(4)	2.588(7)	Br(2)–Cd–Br(3)	105.0(2)
N(1)–C(2)	1.62(7)	Br(2)–Cd–Br(4)	104.4(2)
N(1)–C(5)	1.39(6)	Br(3)–Cd–Br(4)	118.8(2)
N(2)–C(1)	1.46(7)	C(2)–N(1)–C(5)	114(3)
N(2)–C(4)	1.21(5)	C(4)–C(2)–N(1)	112(3)
C(1)–C(5)	1.28(7)	N(1)–C(5)–C(1)	127(4)
C(2)–C(4)	1.54(7)	N(2)–C(1)–C(5)	116(5)
C(1)–C(7)	1.49(8)	C(1)–N(2)–C(4)	128(4)
C(2)–C(8)	1.43(7)	C(2)–C(4)–N(2)	120(3)
C(4)–C(6)	1.51(6)		
C(5)–C(3)	1.57(5)		

Short contacts in **2**[b]

Connection	d(N···Br)	d(H···Br)	∠(N–H···Br)
N(2)–H(14)···Br(2)	3.31(3)	2.83	112
N(2)–H(14)···Br(4)[#1]	3.27(4)	2.42	150
N(1)–H(13)···Br(3)[#2]	3.16(4)	2.40	136
N(1)–H(13)···Br(2)[#3]	3.23(4)	2.67	118

[b] #1: x, y, $-1+z$; #2: $-x$, $1/2+y$, $3/2-z$; #3: $-x$, $1/2+y$, $1/2-z$.

Regarding the cation, the nitrogen base may be protonated to give the 4-pyridylammonium $[H_3NC_5H_4N]^+$ or the 4-aminopyridinium $[H_2NC_5H_4NH]^+$ form in the crystal structure. MO calculations have predicted $[H_3NC_5H_4N]^+$ to be more stable than $[H_2NC_5H_4NH]^+$ [10]. However, the 4-aminopyridinium cation $[H_2NC_5H_4NH]^+$ has recently been found in the crystal structure of 4-aminopyridinium tetrabro-

Table 3. ^{81}Br NQR frequencies at several temperatures.

Compound	ν (MHz) (77 K)		ν (MHz) (273 K)		Intensity ratio	Assignment
1	68.24	averaged	66.61	averaged	1	Br(3)
	65.59	66.31[a]	62.73	64.51[a]	1	Br(1)
	63.18		62.09		2	Br(2)
2	65.83	averaged	65.18	averaged	1	Br(1)
	64.53	63.40	62.25	61.99	1	Br(3) or Br(4)
	63.15		61.37		1	Br(3) or Br(4)
	60.07		59.16		1	Br(2)

[a] Weighted average value in consideration of intensity ratio.

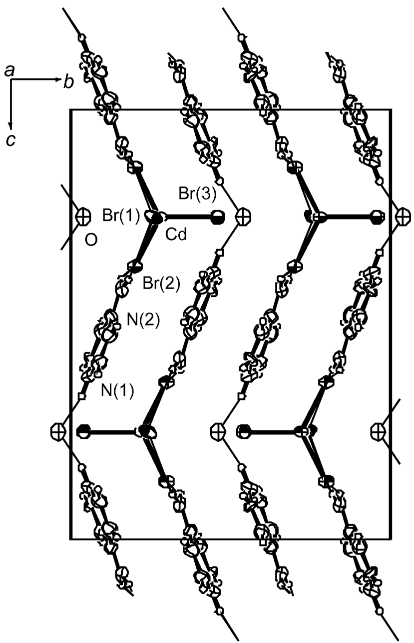

Fig. 1. The projection of the unit cell of **1** along [100] onto the *bc* plane. Hydrogen bonds are shown with thin lines.

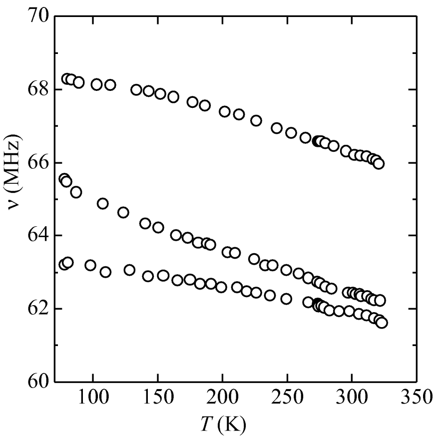

Fig. 2. The temperature dependence of the ^{81}Br NQR frequencies of **1**.

moantimonate [11]. Our crystal structure refinement indicated the presence of 4-aminopyridinium cations in **1**. This cation should also be preferred from a standpoint of crystal stabilization, because both pyridinium and amino NH_2 hydrogen atoms in this form may participate in intermolecular (inter-ionic) hydrogen bonds with the water molecule and with the anion. We thus concluded that our crystals contain the 4-aminopyridinium cation. The possible hydrogen bonds are listed in Table 2.

As described above, $[H_3N(CH_2)_3NH_3][CdBr_4]$ and $[n\text{-}CH_3CH_2CH_2NH_3]_2[CdBr_4]$ [6] crystallize with perovskite-type layered structures of $[CdBr_4{}^{2-}]_\infty$, formed by $CdBr_6$ octahedra sharing four corners. The cations are fitted into the rectangular cavities of the layer sheets with a side length of *ca.* 5.5 Å which is the sum of intra- and interionic bond lengths Br–Cd···Br. In the case of $[H_3NC_6H_4NO_2]_2[CdCl_4]$ [12], the 4-nitroanilinium cation $[H_3NC_6H_4NO_2]^+$ is localized in the cavities with a side length of *ca.* 5.3 Å corresponding to the length of the unit Cl–Cd···Cl. Though the 4-aminopyridinium $[H_2NC_5H_4NH]^+$ cation is compatible in dimension for fitting the cavities with a Br–Cd···Br framework, in reality discrete $CdBr_4{}^{2-}$ anions exist in **1**.

The temperature dependence of the ^{81}Br NQR frequencies of **1** measured between 77 and *ca.* 325 K is shown in Fig. 2. The frequencies at several temperatures are listed in Table 3. The signal intensity ratio among three NQR lines was 1 : 1 : 2, which are denoted as ν_1, ν_2, and ν_3 in decreasing frequency order. The number and intensity ratio of the NQR lines are consistent with three non-equivalent types of Br atoms in the crystal. All the resonance lines exhibited continuous changes of frequency *vs.* temperature without showing any sign of the occurrence of phase transitions. It is noticed that ν_2 exhibits an unusual upward curvature at low temperatures, and its temperature variations are the largest of the three lines.

Though the ^{81}Br NQR frequencies are usually proportional to *d*(Cd–Br), there are no significant differences in the Cd–Br bond lengths with 2.589 ± 0.003 Å. ν_3 with its double intensity is unambiguously assigned to the two equivalent Br(2) atoms of a $CdBr_4{}^{2-}$ anion which are related by a mirror plane. As listed in Table 2, these atoms participate in two N–H···Br hydrogen bonds towards the amino group with the distances of H···Br 2.69 and 2.76 Å. The Br(1) atom participates in two N–H···Br hydrogen bonds with 2 × 3.05 Å. On the other hand, the Br(3) atoms do not participate in any hydrogen bonds. It is well known that hydrogen bonds Br···H usually reduce the NQR frequencies of the relevant Br atoms. With the same argument ν_2 and ν_1 are assigned to the hydrogen bonded Br(1) and the non-hydrogen bonded Br(3) atoms, respectively. In contrast with the Bayer theory [13], which states that NQR frequencies decrease monotonously with increasing temperatures, ν_2 behaves unusually at low temperatures. This may be an indication that the Br(1) atoms take part in another hydrogen bond, Br···H–O, with a water molecule. A short Br(1)···O(1) contact of 3.47 Å is found. In that case the motions of the water molecules modulate preferentially the electric field gradients at the Br(1) nuclei, which may result in the unusual temperature dependence of ν_2 at low temperatures.

DSC measurements were done above r. t. For the first heating runs up to 573 K, an endothermic peak appeared at 390 ± 3 K, and melting was observed at 506 – 524 K. A peak at *ca.* 390 K seems to be composed of several overlapping peaks. Its transition entropy is quite large for a solid-solid phase transitions. These observations indicate that a loss of interstitial water molecules may occur around 390 K on heating.

In the cooling runs, no heat anomaly was observed. In the successive second heating runs two peaks appeared around 390 K, from which ΔH_{tr} = 12.9 kJ mol^{-1} was estimated in total. On further heating, a larger peak with $\Delta H_{\mathrm{tr}} = 17.6 \pm 1.0$ kJ mol^{-1} ($\Delta S_{\mathrm{tr}} = 37.3 \pm 2.0$ J K^{-1} mol^{-1}, $\Delta T = 21 \pm 1$ K) appeared at 473 K, preceding melting with $\Delta H_{\mathrm{tr}} \sim 0.3$ kJ mol^{-1} around 525 K. The second heating run was reproducible for each run.

*2,3,5,6-Tetramethylpyrazinium tetrabromocadmate(II) [2,3,5,6-(CH$_3$)$_4$C$_4$N$_2$H$_2$][CdBr$_4$] (**2**)*

The crystal structure data of **2** are given in Table 1 [9]. The unit cell is shown as a projection along [001] onto the *ab* plane in Fig. 3. The bond lengths, angles and short contacts are included in Table 2. The crystal structure consists of a slightly distorted tetrahedral CdBr$_4$$^{2-}$-anion with four non-equivalent Br atoms and a tetramethylpyrazinium cation. This structure is not isomorphous with that of the corresponding iodide, [2,3,5,6-(CH$_3$)$_4$C$_4$N$_2$H$_2$][CdI$_4$] which crystallizes in the monoclinic space group $P2_1/c$ [14]. However, some similarity is found in the packing of cations and anions. The units are comprised of ion pairs of [2,3,5,6-(CH$_3$)$_4$C$_4$N$_2$H$_2$]$^{2+}$ and CdX$_4$$^{2-}$ related by the 2_1 screw axes along the *a*, *b* and *c* axes in the structure of the bromide. The bifurcated N–H···Br hydrogen bonds between the ion pairs result in infinite series along the *b* axis. On the contrary, in the structure of the iodide, only one 2_1 screw axis exists along the *b* axis, along which the ion pairs are connected by the bifurcated N–H···I hydrogen bonds into infinite series. Though [2,3,5,6-(CH$_3$)$_4$C$_4$N$_2$H$_2$]$^{2+}$ is almost equal in its dimensions to [H$_3$NC$_6$H$_4$NO$_2$]$^+$ which fits into the square column holes of the anion sheets of [H$_3$NC$_6$H$_4$NO$_2$]$_2$[CdCl$_4$] [12], it prefers to make the ion pairs without allowing an aggregation of anions into sheets.

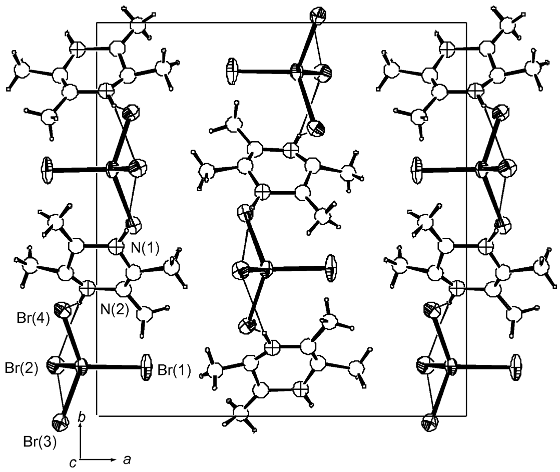

Fig. 3. The projection of the unit cell of **2** onto the *ab* plane along [001]. Hydrogen bonds are shown with thin lines.

The temperature dependence of the ^{81}Br NQR frequencies for **2** measured between 77 and about 330 K is shown in Fig. 4. Four NQR lines, which are denoted as ν_1, ν_2, ν_3, and ν_4 in decreasing frequency order, with the intensity ratio of 1 : 1 : 1 : 1 appear throughout the observed temperature range. All resonance lines exhibit continuous normal changes of frequencies *vs.* temperatures without showing any signs of the occurrence of phase transitions. The ^{81}Br NQR frequencies at several temperatures are listed in Table 3. The number of NQR lines is consistent with the four non-equivalent Br atoms in the crystal. The averaged ^{81}Br NQR frequency of **2** is shifted to the

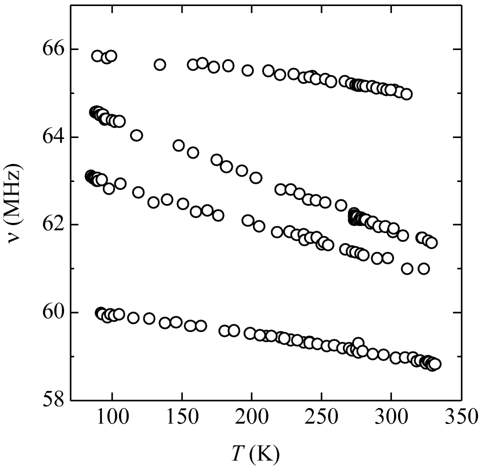

Fig. 4. The temperature dependence of the ^{81}Br NQR frequencies of **2**.

low frequency side by *ca.* 2.5 MHz from that of **1** as listed in Table 3. This may be an indication of stronger hydrogen bonds N–H···Br with the bivalent cations in **2** than with the monovalent cations in **1** as shown in Table 2.

The temperature dependence curves of the ^{81}Br NQR lines in Fig. 4 are classified into two groups, (ν_1, ν_4) and (ν_2, ν_3), with weak and strong temperature dependence, respectively. The highest frequency line ν_1 may be assigned to the Br(1) atom when considering that this atom has the shortest bond Cd–Br(1) and does not engage in hydrogen bonds N–H···Br. The lowest frequency line ν_4 may be assigned to Br(2), which is connected by two short hydrogen bonds. The middle two lines (ν_2, ν_3) then remain for the Br(3) and Br(4) atoms and are difficult to assign owing to similar environments. These tentative assignments are included in Table 3.

The DSC measurements showed the occurrence of a phase transition at 522.5 ± 1.0 K with a ΔH_{tr} of 0.3 kJ/mol. This transition is considered to be a displacive-type on judging from its small ΔH_{tr}. Upon a further increase in temperature, decomposition of the compound occurred just below the melting point of about 590 K.

Experimental Section

*[4-$H_2NC_5H_4NH]_2[CdBr_4]\cdot H_2O$ (**1**)* was prepared by mixing 4-aminopyridine and cadmium(II) carbonate in the molar ratio 2 : 1 in concentrated hydrobromic acid. The crude product was recrystallized from water as colorless prisms. Pink crystals were obtained from concentrated hydrobromic acid solution, but they exhibited exactly the same structure as shown by X-ray structure determinations.

*[2,3,5,6-$(CH_3)_4C_4N_2H_2][CdBr_4]$ (**2**)* was obtained as yellow plate-like crystals by mixing 2,3,5,6-tetramethylpyrazine and cadmium(II) carbonate in the molar ratio 1 : 1 in dilute hydrobromic acid solution adjusted to pH ≈ 2. For recrystallization the solution was kept in a desiccator charged with P_2O_5. Analysis for **1**: calcd. C 18.69, H 2.82, N 8.72; found C 18.82, H 2.57, N 8.77. **2**: calcd. C 16.85, H 2.47, N 4.91; found C 16.87, H 2.46, N 4.82.

The crystal structures were determined using a four-circle X-ray diffractometer Rigaku AFC5S (MoK_α radiation, λ = 0.7107 Å, graphite monochromator, attenuator: Zr foil; $\omega/2\theta$ scans). The hydrogen atom positions were calculated with standard bond lengths and angles. For **1** both possible cations, the 4-pyridylammonium cation $[H_3NC_5H_4N]^+$ and the 4-aminopyridinium cation $[H_2NC_5H_4NH]^+$, were refined giving better results for the 4-aminopyridinium cation [9]. All calculations were performed using the CRYSTALSTRUCTURE crystallographic software package [15].

Differential Scanning Calorimetry (DSC) measurements were performed above r. t. with a DSC220 apparatus from Seiko Instruments Inc. under the following conditions: sample weight *ca.* 10 mg, heating or cooling rates 2 – 10 K min^{-1} with flowing dry N_2 gas at 40 mL min^{-1}.

Nuclear quadrupole resonance (NQR) spectra were obtained with a homemade super-regenerative spectrometer and recorded through a lock-in amplifier with Zeeman modulation. The ^{81}Br NQR lines observed were identified by observing the corresponding ^{79}Br lines in the known frequency ratio.

---

[1] H. Ishihara, S. Dou, K. Horiuchi, V. G. Krishnan, H. Paulus, H. Fuess, A. Weiss, *Z. Naturforsch.* **1996**, *51a*, 1027 – 1036.

[2] H. Ishihara, K. Horiuchi, S. Dou, T. M. Gesing, J. C. Buhl, H. Paulus, H. Fuess, *Z. Naturforsch.* **1998**, *53a*, 717–724.

[3] H. Ishihara, V. G. Krishnan, S. Dou, H. Paulus, A. Weiss, *Z. Naturforsch.* **1994**, *49a*, 213–222.

[4] H. Ishihara, K. Horiuchi, S. Dou, T. M. Gesing, J. C. Buhl, H. Paulus, I. Svoboda, H. Fuess, *Z. Naturforsch.* **1999**, *54a*, 628–636.

[5] H. Ishihara, K. Horiuchi, V. G. Krishnan, I. Svoboda, H. Fuess, *Z. Naturforsch.* **2000**, *55a*, 390–396.

[6] H. Ishihara, S. Dou, K. Horiuchi, V. G. Krishnan, H. Paulus, H. Fuess, A. Weiss, *Z. Naturforsch.* **1996**, *51a*, 1216–1228.

[7] H. Ishihara, K. Horiuchi, T. M. Gesing, S. Dou, J. C. Buhl, H. Terao, *Z. Naturforsch.* **2000**, *55a*, 225–229.

[8] H. Ishihara, K. Horiuchi, T. M. Gesing, S. Dou, J. C. Buhl, P. Erk, *Z. Naturforsch.* **2002**, *57b*, 503–508; H. Ishihara, N. Hatano, K. Horiuchi, H. Terao, *Z. Naturforsch.* **2002**, *57a*, 343–347; H. Ishihara, K. Horiuchi, I. Svoboda, H. Fuess, T. M. Gesing, J. C. Buhl, H. Terao, *Z. Naturforsch.* **2006**, *61b*, 69–72.

[9] CCDC 686234 (**1**) and 686235 (**2**) contain the supplementary crystallographic data for this paper. These data can be obtained free of charge from The Cambridge Crystallographic Data Centre *via* www.ccdc.cam.ac.uk/ data_request/cif.

[10] The formation energies were calculated by PM3 calculation using WINMOPAC (version 3), Fujitsu Limited, **1997 – 2000**

[11] M. Hashimoto, H. Terao, H. Fuess, I. Svoboda, H. Ehrenberg, *Bull. Chem. Soc. Jpn.* **2003**, *76*, 749–753.

[12] R. Azumi, K. Honda, M. Goto, J. Akimoto, Y. Oosawa, H. Tachibana, T. Nakamura, M. Tanaka, M. Matsumoto, *Acta Cryst.* **1995**, *C51*, 2534–2537.

[13] H. Bayer, *Z. Physik* **1951**, *130*, 227–238.

[14] D. B. Rosa, T. P. William, *Acta Cryst.* **1995**, *C51*, 226–229.

[15] CRYSTALSTRUCTURE (version 3.7.0), Crystal Structure Analysis Package, Rigaku and Rigaku/MSC, **2000 – 2005**.